

1 HOW DROUGHT SEVERITY CONSTRAIN GPP AND ITS PARTITIONING
2 AMONG CARBON POOLS IN A *QUERCUS ILEX* COPPICE?
3

4 Rambal S^{1, 5}, Lempereur M^{1, 6}, Limousin JM², Martin-StPaul NK^{1, 3, 7}, Ourcival JM¹,
5 Rodríguez-Calcerrada J⁴

6
7 ¹Centre d'Ecologie Fonctionnelle et Evolutive CEFE, UMR 5175, CNRS - Université de
8 Montpellier - Université Paul-Valéry Montpellier – EPHE 1919 Route de Mende, 34293
9 Montpellier Cedex 5, FRANCE

10 ²Department of Biology, University of New Mexico, MSC03 2020, Albuquerque, New
11 Mexico 87131-0001, USA

12 ³Laboratoire Ecologie Systématique et Evolution CNRS, Orsay, F-91405, France

13 ⁴Grupo de Investigación en Genética y Fisiología Forestal, E.T.S.I. Montes, Universidad
14 Politécnica de Madrid. Ciudad Universitaria S/N. 28040 Madrid, España

15 ⁵Universidade Federal de Lavras, Departamento de Biologia, CP 3037, CEP 37200-000,
16 Lavras, MG, Brazil

17 ⁶Agence de l'Environnement et de la Maîtrise de l'Energie 20, avenue du Grésillé- BP 90406
18 49004 Angers Cedex 01 France

19 ⁷INRA, URFM, Ecologie des Forêts Méditerranéennes, UR 629, Domaine Saint Paul, Site
20 Agroparc, F-84914 Avignon Cedex 9, France

21

22 **ABSTRACT**

23 The partitioning of photosynthates toward biomass compartments has a crucial role in the
24 carbon sink function of forests. Few studies have examined how carbon is allocated toward
25 plant compartments in drought prone forests. We analyzed the fate of *GPP* in relation to
26 yearly water deficit in an old evergreen Mediterranean *Quercus ilex* coppice severely affected
27 by water limitations. , Carbon fluxes between the ecosystem and the atmosphere were
28 measured with an eddy-covariance flux tower running continuously since 2001. Discrete
29 measurements of litterfall, stem growth and f_{APAR} allowed us to derive annual productions of
30 leaves, wood, flowers and acorns and an isometric relationship between stem and
31 belowground biomass has been used to estimate perennial belowground growth. By
32 combining eddy-covariance fluxes with annual productions (*NPP*), we managed to close a C
33 budget and derive values of autotrophic, heterotrophic respirations and carbon use efficiency
34 (*CUE*, the ratio between *NPP* and *GPP*). Average values of yearly *NEP*, *GPP* and R_{eco} were
35 282, 1259 and 977 g C m⁻². The corresponding *ANPP* components were 142.5, 26.4 and
36 69.6 g C m⁻² for leaves, reproductive effort (flowers and fruits) and stems. *NEP*, *GPP* and R_{eco}
37 were affected by annual water deficit. Partitioning to the different plant compartments was
38 also impacted by drought, with a hierarchy of responses going from the most affected, the
39 stem growth, to the least affected, the leaf production. The average *CUE* was 0.40, which is
40 well in the range for Mediterranean-type forest ecosystems. *CUE* tended to decrease more
41 slightly in response to drought than *GPP* and *NPP*, probably due to drought-acclimation of
42 autotrophic respiration. Overall, our results provide a baseline for modeling the inter-annual
43 variations of carbon fluxes and allocation in this widespread Mediterranean ecosystem and
44 highlight the value of maintaining continuous experimental measurements over the long term.
45

46 **1. INTRODUCTION**

47 Forest ecosystems exert a strong influence on the global C cycle (Bonan, 2008) as forests may
48 contribute up to 60% of the total land carbon uptake (Beer et al., 2010). Estimations and
49 simulations of carbon uptake by forest ecosystems have been greatly improved in recent
50 decades, but unfortunately how this assimilated C is transferred from the atmosphere to the
51 terrestrial biomass remains poorly known. Luo et al. (2011) highlighted a lack of mechanistic
52 understanding on this question and suggested “to develop generalizable models of C
53 allocation to biomass growth of plant parts, respiration, nonstructural C reserve, reproduction
54 and defense” as a challenging issue. A recent synthesis has demonstrated that the partitioning
55 of gross photosynthetic production (*GPP*) among above- and below-ground production and
56 respiration can vary greatly across biomes according to climate and fertility (Litton and
57 Giardina, 2008). However, a more detailed understanding of how environmental factors affect
58 the distribution of C among the different tree parts at the ecosystem scale remains a crucial
59 step to improve the accuracy of local and global vegetation models (Fatichi et al., 2013;
60 Leuzinger and Quinn Thomas, 2011).

61 Understanding C allocation patterns appears particularly important in drought prone
62 areas, such as those with a Mediterranean-type climate, which are particularly vulnerable to
63 the ongoing climate change (Giorgi, 2006). According to global and regional climate models,
64 Mediterranean-type ecosystems (MTEs) will suffer longer and more intense droughts as a
65 result of 1) increasing temperature and decreasing rainfall (Hoerling et al., 2011), 2) a change
66 in large-scale circulation conditions (Kjellström et al., 2013), and 3) the persistence of heat
67 wave anomalies (Jaeger and Seneviratne, 2011). In MTEs, drought is already the prevailing
68 constraint on the net ecosystem productivity (*NEP*) (Allard et al., 2008; Grünzweig et al.,
69 2003). This sink strength is likely modified by the differential sensitivity to water limitation of
70 leaf photosynthesis and whole-tree respiration, and of the C allocation to short- and long-lived
71 pools. The representation of C use in models currently lacks consensus and is achieved by a
72 plethora of concurrent approaches (Franklin et al., 2012). This modeling deficiency seems to
73 be due to the difficulty in interpreting this information in generic schemes that are valid under
74 a wide range of conditions, and particularly water limitation.

75 So far, studies addressing the question of C-use in MTEs have relied on the coupling
76 of field data of standing biomass and growth compartments with simulation models.
77 Pioneering works started in the 70s onwards (Eckardt et al., 1975). Oechel and Lawrence
78 (1981) applied the process-based model MEDECS to eight woody Mediterranean species

79 growing in California chaparral and Chilean matorral. The model scaled up leaf level
80 respiration and assimilation together with stem respiration to yield yearly C budgets using a
81 radiation transfer scheme. The hierarchy of C allocation to leaves, stems, and roots followed
82 species-specific rules and a phenological calendar. From this modeling exercise, the authors
83 deduced changes in C use that deeply modified the respiratory costs in response to changes in
84 air temperature. Yet, the effect of drought on C use remains more difficult to understand and
85 simulate.

86 Forests and woodlands dominated by the evergreen oak *Quercus ilex* L. occupy large
87 areas in the surrounding of the Mediterranean Sea (Quézel and Médail, 2003) and are
88 emblematic of the MTEs. Due to its resprouting nature, *Q. ilex* can persist in the same place
89 for hundreds of years and populations display minimal changes in stool number per area. Very
90 large survival rates and fast recovery of its foliage after complete dieback (Lloret et al., 2004)
91 reflect its high ability to damp climate extremes (Misson et al., 2011). In contrast, co-
92 occurring obligate seeders are subjected to all the vicissitudes of regeneration, and are
93 particularly affected by drought mortality at the seedling stages and by wildfires (Ackerly,
94 2004; Zavala, 1999). The growing interest in resprouting ability as a major plant functional
95 trait is reflected in a number of recent contributions aimed at understanding the biogeography
96 and developing functional models of resprouting species (Clarke et al., 2010; Vesk and
97 Westoby, 2004; Vilagrosa et al., 2014). Resprouters have the particularity to store
98 considerable amounts of C belowground at the cost of high maintenance respiration (Iwasa
99 and Kubo, 1997). Characterizing the ecosystem C use for such species is important for
100 managing and predicting the response of Mediterranean forests to the on-going climate
101 changes.

102 The functioning of *Quercus ilex* stands in Southern France was simulated by Hoff et
103 al. (2002) and Hoff and Rambal (2003) using the Forest-BGC model. C-use rules in this
104 simple model are implemented so as to follow an optimal trajectory: trees use C first into
105 leaves and fine roots for maximizing productivity while minimizing water limitation; finally
106 stems appear as an end-product built with the remaining C. Other modeling exercises with *Q.*
107 *ilex* ecosystems also retained water-related constraints for their C-use rules. Gracia et al.
108 (1999) developed a dynamic growth model where the partitioning of growth between leaves
109 and perennial wood compartments is performed so as to fulfill the assumptions of the pipe
110 model theory (Shinozaki et al., 1964; see also Mäkelä, 1986 for substantial accounts;
111 Valentine, 1985), i.e. so as to maintain the sap area/foliage area ratio constant. Gracia et al.
112 (1999) also constrain growth to fine roots to follow the functional balance hypothesis

113 (Brouwer, 1962). Both abovementioned modeling exercises yielded credible results when
114 validated against yearly variations of radial growth. Fortunately, the increasing availability of
115 long term field measurements of productivity and eddy covariance fluxes can now help to
116 refine these previous modeling hypotheses.

117 In this study, our main objectives were: 1) to evaluate the fraction of *GPP* partitioned to
118 above- and below-ground parts in a *Quercus ilex* forest by comparing different ecosystems
119 across a range of climate, management, and drought resistance of dominant species, and 2) to
120 assess how year-to-year variation in drought severity impacts the partitioning of *GPP* between
121 production and respiration, and among above- and below-ground C pools. For these purposes,
122 we used long-term data of eddy covariance fluxes and primary productivity of aboveground
123 components (leaves, flowers, fruits and stems), plus punctual data of root biomass taken from
124 literature and our own excavation of four *Q. ilex* trees.

125

126 2. MATERIAL AND METHODS

127 2.1. Site description

128 The study site is located 35km north-west of Montpellier (southern France), on a flat plateau
129 in the Puéchabon State Forest (3°35'45"E, 43°44'29"N, 270m a.s.l.). This forest has been
130 managed as a coppice for centuries and the last clear cut was performed in 1942. Vegetation is
131 largely dominated by a dense overstorey of the evergreen oak *Quercus ilex*. The top canopy
132 height is about 5.5m. In 2010, stem density was 4900 stems·ha⁻¹. Stems with diameter at
133 breast height (*DBH*) < 4cm represented 6 % of total stems, whereas those with *DBH* > 10cm
134 represented 20.6 %. Understorey species *Buxus sempervirens*, *Phyllirea latifolia*, *Pistacia*
135 *terebinthus* and *Juniperus oxycedrus*, compose a sparse shrubby layer with a percent cover
136 lower than 25% and a height less than 2 m.

137 The area has a Mediterranean-type climate. Rainfall mainly occurs during autumn and
138 winter, with about 80% taking place between September and April. The mean annual
139 precipitation is 916 mm, with a range of 556-1549 mm recorded over the 1984-2011 period.
140 Mean annual temperature over the same period was 13.0°C, with a minimum in January
141 (5.5°C) and a maximum in July (22.9°C). The rocky soil is formed on Jurassic limestone; on
142 average, the volumetric fractional content of stones and rocks is about 0.75 for the top 0-50
143 cm and 0.90 below. The stone-free fine fraction of the soil is a homogeneous silty clay loam
144 (USDA texture triangle) within the top 0-50cm layer (38.8% clay, 35.2% silt and 26% sand).
145 The fine fraction fills up the space between stones and rocks and provides a source of water
146 throughout the long dry summers for the deep-rooted *Q. ilex* (Rambal, 2011). The highly
147 permeable soil prevents any surface runoff to occur even for high intensity rain events.

148

149

150 2.2. Water limitation: Soil water balance model and drought index

151 Soil water storage integrated over the rooting depth, that is c.a. 4.5 m (Rambal, 2011), has
152 been measured during the vegetative periods of 1984-1986 and since July 1998 onwards, at
153 approximately monthly intervals, using a neutron moisture gauge (see Hoff et al., 2002).
154 Discrete measurements were interpolated at a daily time step with a soil water balance model
155 proposed in Rambal (1993) and further used in Grote et al. (2009). The drainage curve
156 relating deep drainage to soil water storage depends on the stone content over the whole-soil
157 profile (Rambal, 1990). The model was driven by daily values of incoming solar radiation,
158 minimal and maximal temperature and rain amount. Soil water storage and soil water

159 potential were related by a Campbell-type retention curve (Campbell, 1985) whose
160 parameters are strongly dependent on soil texture (see details in Rambal et al., 2003).
161 Comparison of measured against simulated values of soil water storage (in mm), and predawn
162 leaf water potential (in MPa), displayed very good agreement. Leaf water potential values
163 came from discrete measurements performed on the study site (see Limousin et al., 2012 for a
164 substantial account). For soil water storage, reduced major axis (RMA) regressions yielded
165 $SWS_{sim} = \alpha_{rma} SWC_{obs} + \beta_{rma}$ with $\alpha_{rma} \pm \text{standard-error (SE)} = 0.94 \pm 0.03$, $\beta_{rma} \pm \text{SE} = 6.0 \pm 4.4$,
166 $R^2 = 0.93$, $F = 1137$, $p < 0.0001$ and $n = 91$; for the predawn potential, $\psi_{pdsim} = \alpha_{rma} \psi_{pdobs} +$
167 β_{rma} with $\alpha_{rma} \pm \text{SE} = 0.93 \pm 0.05$, $\beta_{RMA} \pm \text{SE} = -0.09 \pm 0.09$, $R^2 = 0.840$, $F = 273.3$, $p < 0.0001$
168 and $n = 54$. The continuous daily course of relative water content, RWC , was derived from
169 SWS_{sim} divided by the soil water storage at field capacity that we chose to fix at 205 mm. This
170 value corresponds to that observed after 2 days of free drainage in a cool wet period after a
171 substantial rain event. For characterizing the whole-year water limitation, we calculated the
172 water stress integral (WSI) as the yearly sum of ψ_{pdsim} . For days with $RWC \geq 1$ ψ_{pdsim} is fixed
173 to -0.03 MPa. The WSI are expressed in MPa day.

174

175 **2.3. Drought frequency analysis**

176 The return periods for drought events were calculated, using a monthly 239-year precipitation
177 historical dataset (1762-2011) for Montpellier downtown. This dataset was scaled to our
178 experimental site using overlapping precipitation data from 1984 to 2011. As shown by
179 Rambal and Debussche (1995) and López-Moreno et al. (2009), the coefficient of variation
180 for precipitation is regionally conserved and was used to fit theoretical lognormal distribution
181 functions for extreme precipitation events at our site. Return periods were calculated as $1/p$,
182 where p is the probability of occurrence (Rambal and Debussche, 1995).

183

184 **2.4. Carbon fluxes and ancillary data**

185 Daily climate data, further used as model inputs for a water budget model, came from a
186 weather station located 200 m away from the flux tower.

187 Eddy covariance fluxes of CO_2 , sensible heat, latent heat and momentum were
188 measured continuously since 2001 at the top of a 12 m high tower that is approximately 6 m
189 above the canopy. Our eddy covariance facility included a three-dimensional sonic
190 anemometer (Solent R3, Gill Instruments, Lymington, England) and a closed path infrared gas
191 analyser (IRGA, model LI 6262, Li-Cor Inc., Lincoln, Nebraska, USA), both sampling at a

192 rate of 21Hz. Flux data were processed with protocols defined within the Carbo-Europe
 193 network (www.carboeurope.org, Aubinet et al., 2000). Processing schemes of Fluxnet have
 194 been used for filling data gaps and partitioning *NEP* into *GPP* and ecosystem respiration *R_{eco}*
 195 (Papale, 2006; Reichstein et al., 2005). The half-hourly fluxes were summed at a yearly time
 196 steps for further analysis. Photosynthetically active radiation *PAR_{top}* was recorded at the top of
 197 the flux tower. The fraction of PAR absorbed by the canopy (*f_{APAR}*) was derived from 14 *PAR*
 198 sensors randomly set up in understorey locations and measuring *PAR_{below}*:

$$f_{APAR} = 1 - PAR_{below}/PAR_{top} \quad (1)$$

199

200 **2.5. Leaf production and other growth components**

201 *ANPP_{stem}* was estimated from yearly measurements of stem *DBH* and the allometric
 202 relationship between stem biomass and stem *DBH*. *ANPP_{leaf}* and *ANPP_{reprod}* were derived
 203 from monthly litter falls measured on 26 x 0.141 m² litter traps. *ANPP_{reprod}* comprised
 204 flowers and acorns. *ANPP_{leaf}* was derived by estimating yearly changes of leaf mass at peak
 205 leaf area index plus the amount of leaves lost as litter. Leaf production in year *t* occurred from
 206 May to June and *M_{leaflitter}* was calculated as the sum of monthly values of leaf litter fallen from
 207 August *t-1* to July *t*. *M_{leaflitter}* was corrected for mass loss at abscission using the results of
 208 Cherbuy et al. (2001):

$$ANPP_{leaf} = M_{leaf}(t) - M_{leaf}(t - 1) + M_{leaflitter} = \Delta M_{leaf} + M_{leaflitter} \quad (2)$$

209 Peak *LAI = PAI - SAI* was estimated from continuous measurements of half-hourly
 210 *f_{APAR}* between 11 AM and 1 PM from DOY 205 to 225. We first derived the plant area index
 211 *PAI* by using a Beer's Law with an extinction parameter equal to $k/\sin\beta$. The parameter *k* was
 212 set to 0.72 as in Rambal et al. (2003) and β is the solar elevation angle. The Stem Area Index
 213 *SAI* was estimated by image processing of hemispheric photography. It was assumed constant
 214 for the whole period and equal to 0.5 (Poncelet unpublished data). *LAI* was converted to leaf
 215 mass with a canopy-averaged leaf mass per area of 215 g m⁻² (see Rambal et al., 1996). The
 216 below-canopy *PAR* sensor network was set up in 2001 so the leaf production for 2001 was not
 217 available. Even though *Q. ilex* is a strong emitter of terpenoids (Staudt et al., 2002), biogenic
 218 volatile compound emissions are relatively minor C sources and they were neglected here. So,
 219 the aboveground net productivity was computed as:

$$ANPP = ANPP_{leaf} + ANPP_{stem} + ANPP_{reprod} \quad (3)$$

221 In 2005 we observed a massive outburst of *Lymantria dispar*. Grazing from
 222 caterpillars drastically impacted the leaves so we decided to exclude data from this year in our

223 calculations. Data for the belowground perennial components were obtained by excavating
 224 four stumps at our site, and from literature values published by Canadell and Roda (1991) and
 225 Djema (1995) for *Q. ilex* coppices growing in northeast Spain under similar climate
 226 conditions. We compiled 19 biomass values for root crown, roots greater than 5 cm, and roots
 227 ranging from 1 to 5 cm diameter. The whole perennial belowground compartment is the sum
 228 of root crown and large roots. We obtained an isometric relationship between stem and
 229 belowground biomass, with a slope equal to 1.068 ± 0.1235 ($s_{x,y} = 62.2$, $n=19$, $p<0.001$) (Fig.
 230 A1). All these data came from excavations in very stony soils and only concerned the top 0-1
 231 m layer. A significant part of the root system was not extracted because we have observed that
 232 tap roots are able to uptake soil water at depths ranging between four and five meters
 233 (Rambal, 2011). We thus applied a conservative correction factor of 10% to account for the
 234 missing root part. Our belowground to aboveground ratio could be considered constant
 235 whatever the stool size, so we propose an isometric partition of C between these two perennial
 236 compartments. We postulate that the error we made in estimating $BNPP_{coarse}$ is equivalent to
 237 the one we made in evaluating the change in stem biomass:

$$238 \quad ANPP_{stem} = \alpha BNPP_{coarse} \quad (4),$$

239 with $BNPP$ representing belowground net primary productivity. Fine root production was
 240 taken from literature values. López et al. (2001a) extensively monitored fine root productivity
 241 in a *Q. ilex* coppice. They found annual fine root production over the 0-60 cm soil layer to be
 242 quasi identical to leaf production (average fine root to leaf production ratio over two years
 243 was 1.04). We correct this value for the whole profile using a ratio of 1.25, based on the
 244 distribution of fine roots over the soil profile proposed by Jackson et al. (1997) for
 245 sclerophyllous shrubs and trees, and the increase in fine root turnover rate with depth (López
 246 et al., 2001b):

$$BNPP = BNPP_{coarse} + BNPP_{fine} \quad (5)$$

247 Biomasses were converted to C using tissue-specific C contents whenever available; else 0.48
 248 was used as a default.

249

250 **2.6. Carbon budget estimate**

251 The different components of the carbon budget were related to each other according to three
 252 identities considered here as yearly sums (Fig. 1):

$$NPP = ANPP + BNPP = GPP - R_a \quad (6)$$

$$NEP = NPP - R_h = GPP - R_{eco} \quad (7)$$

$$R_{eco} = R_a + R_h \quad (8)$$

253 R_a is the autotrophic respiration, including both growth and maintenance components, with
254 R_{aa} and R_{ab} standing for the above- and below-ground parts, respectively. R_h is the
255 heterotrophic respiration. Uncertainty estimation of fluxes were around $20 \text{ g C m}^{-2} \text{ y}^{-1}$, 30 g C
256 $\text{m}^{-2} \text{ y}^{-1}$ and $40 \text{ g C m}^{-2} \text{ y}^{-1}$ for NEE , GPP and R_{eco} , respectively (Misson et al., 2010; see also
257 Stauch et al., 2008).

$$GPP = ANPP + R_{aa} + TBCF \quad (9)$$

258 Total belowground carbon allocation ($TBCF$) was defined as that carbon allocated
259 belowground by plants to coarse and fine roots production, root respiration, and root exudates
260 and mycorrhizae. $TBCF$ is either respired by microbes or roots (measured as soil-surface CO_2
261 efflux) or stored in soil as organic matter in the litter layer or in living and dead roots.
262 Growth respiration was calculated using the yield of growth processes Y (Thornley, 1970).
263 This yield is the amount of biomass increment per unit of C substrate used in growth
264 processes. It was expressed in g C of new biomass (g C of substrate used in the growth
265 processes)⁻¹. For *Q. ilex* in Puéchabon, the Y parameter has been estimated to 0.8 g C
266 appearing in new biomass per g of C substrate utilized (Rambal et al., 2004). In equations 6, 7
267 and 9, we neglect nonstructural C storage above or belowground. In the carbon budget we
268 wrote an equation in which C balance is zero independently of the water limitation, and
269 consequently the storage of nonstructural C pool remains constant (see Ryan, 2011; Sala et
270 al., 2010; Stauch et al., 2008 for the role of nonstructural carbohydrates in coping with
271 drought).

272

273 3. RESULTS

274 3.1. Environmental conditions and exceptional years

275 Over the study period (2001-2011), annual rain amounts ranged from 638.2 mm in 2007 to
276 1310 mm in 2003. The average value over this period (976.8 mm) was slightly greater than
277 the longer term mean (1984-2011, 916 mm). *WSI* ranged from -112.6 MPa day in the wettest
278 year (2004) to -358.6 MPa day in the driest year (2006). There was no relationship between
279 the annual rainfall amount and the annual *WSI* that the vegetation underwent. Lower *WSI*
280 occurred in years when the dry period began early in the spring season. In the driest year 2006
281 the rain deficit began in February, and from February to June the rainfall amount reached only
282 109.8 mm. We calculated a probability of 0.015 for the 2006 drought, corresponding to a
283 return period of 67 years. Other years with dry spring seasons in the historical series were:
284 1779, 1780, 1817, 1929, 1945 and 1995, but all these years displayed less severe droughts
285 than 2006. So, over the 2001-2011 period, we observed a very large range of water limitation
286 from well-watered conditions to severe drought. There was no significant covariation between
287 mean annual temperature and *WSI*.

288

289 3.2. C fluxes and production

290 The mean gross C input, *GPP*, was $1259 \text{ g C m}^{-2} \text{ yr}^{-1}$ and its coefficient of variation (CV), or
291 between-year variation, was 13.3%. For *NEP* the mean value was $281.7 \text{ g C m}^{-2} \text{ yr}^{-1}$ with a
292 larger CV of 33.5%; and for *R_{eco}* it was $977.2 \text{ g C m}^{-2} \text{ yr}^{-1}$, with a CV = 8.9% (Fig. 2).

293 The average LAI was 2.25 ± 0.2 , which corresponds to a supported leaf mass of
294 231.7 g C m^{-2} ($n = 10$) with a coefficient of variation CV = 9% (Fig. A2.). Our calculation of
295 the leaf production yields an average value of $142.5 \text{ g C m}^{-2} \text{ yr}^{-1}$ ($n = 9$) with a large CV of
296 28.5%. The leaf production ranged from $202.8 \pm 77.1 \text{ g C m}^{-2} \text{ yr}^{-1}$ in 2006, the year after the
297 *Lymantria dispar* outburst and heavy grazing, to $69.6 \pm 58.2 \text{ g C m}^{-2} \text{ yr}^{-1}$ the following year in
298 2007. The reproductive effort, *ANPP_{reprod}*, evaluated in pooling flowers and acorns, displayed
299 the greater between-year variation, with a 42.5% CV, and a mean value of 26.4 g C m^{-2} . The
300 components of *ANPP_{reprod}* were, on average, $11.0 \text{ g C m}^{-2} \text{ yr}^{-1}$ for flowers (CV = 48.5%) and
301 $15.4 \text{ g C m}^{-2} \text{ yr}^{-1}$ for acorns which displayed the largest variation (CV = 87.8%). Summing
302 leaves plus flowers and acorns we obtained an average $169.6 \text{ g C m}^{-2} \text{ yr}^{-1}$, which accounted
303 only for 16.9% of the yearly *GPP*.

304

3.3. Relationships between production components and water limitation

Significant linear declines of GPP , NEP and R_{eco} with increasing drought severity were observed across years (Table 1; Fig. 3). Respectively 72% and 80% of the variance in GPP and NEP was explained by the WSI . The slopes of the $WSI-GPP$ and $-NEP$ lines were 1.91 ± 0.43 and 1.15 ± 0.20 , respectively, which means that we project a decline of GPP of $191 \text{ g C m}^{-2} \text{ yr}^{-1}$ and of NEP of $115 \text{ g C m}^{-2} \text{ yr}^{-1}$ for an increase in drought severity of 100 MPa day expressed in terms of WSI . The sensitivity to drought of R_{eco} was lower than for the two other components of the whole-ecosystem C budget, with a lower slope of 0.77 ± 0.32 associated with a lower explained variance, 42%.

Among the aboveground tree compartments, the most affected by drought was the stem (Fig. 4), with $dANPP_{stem}/dWSI = 0.42 \pm 0.10$ (Table 1; Fig. 4). According to the linear equation fitted between $ANPP_{stem}$ and WSI , the predicted allocation of C to the stem ranged from 120.9 g C m^{-2} for a hypothetical wet year that underwent a WSI of -100 MPa day (WSI in 2004 equaled -112.6 MPa day), to zero in a severely dry year with a WSI of -390 MPa day. Reproduction was also affected by water stress, with $dANPP_{reprod}/dWSI = 0.10 \pm 0.04$ (Fig. 5). In contrast, no significant relationship was found between WSI and $ANPP_{leaf}$ ($p = 0.54$; Table 1; Fig. 6b). $ANPP_{leaf}$ was, however, significantly related to the WSI of the previous year, with a slope of 0.41 ± 0.15 and an explained variance of 52% (Fig. 6a).

3.4. Relationship between CUE and water limitation

By combining the latter results with equations 6 to 9, a model of C use changes with drought severity can be proposed. Fig. 7a depicts the changes of GPP and NPP , and of the above and belowground compartments with WSI . CUE , the ratio of net primary production to gross primary production is also presented. For WSI declining from -100 MPa day in a wet year to -400 MPa day in a particularly dry year, NPP and CUE decline from 621.4 to $339.4 \text{ g C m}^{-2} \text{ yr}^{-1}$ and from 0.419 to 0.373 respectively.

Fig. 7b depicts the declines of R_{eco} and NEP with WSI and the corresponding changes of the ratios of autotrophic respiration to GPP (R_a/GPP) and heterotrophic respiration to whole-ecosystem respiration (R_h/R_{eco}). The R_a/GPP ratio increased from 0.581 to 0.627 for a change of WSI from -100 to -400 MPa day. For the same decline in WSI , the ratio of R_h/R_{eco} increased from 0.192 to 0.321 , with R_h slightly increasing from 205.1 to $268.1 \text{ g C m}^{-2} \text{ yr}^{-1}$.

337 4. DISCUSSION

338 4.1. Carbon use efficiency in a Mediterranean coppice – management and drought- 339 adaptation constraints on carbon allocation rules

340 Carbon use efficiency (*CUE*), the ratio of net primary production (*NPP*) to gross primary
341 production (*GPP*), describes the capacity of forests to assimilate C from the atmosphere into
342 terrestrial biomass. *CUE* of forests has been assumed, by some authors, to be a constant value
343 of 0.47 ± 0.04 (Gifford, 2003; Waring et al., 1998), which supposes that tree respiration is a
344 constant fraction of *GPP*. Contrary to this assumption of constancy, substantial variations in
345 *CUE* have been reported in forest ecosystems. Medlyn and Dewar (1999) demonstrated that
346 *CUE* likely ranges between 0.31 and 0.59, and a more recent synthesis by DeLucia et al.
347 (2007) showed that the slope of the relationship between *NPP* and *GPP* (*CUE*) was 0.53,
348 ranging from 0.23 to 0.83 among forest types. *CUE* decreased with increasing age, and a
349 substantial portion of the variation among forest types was caused by the ratio of leaf mass-to-
350 total mass. For a ratio of leaf mass-to-total mass of 0.03 corresponding to our *Q. ilex* forest,
351 DeLucia et al. (2007) predicted a *CUE* of 0.38, similar to the mean of 0.40 obtained here, and
352 the same value that Oechel and Lawrence (1981) obtained for Californian and Chilean shrub
353 and tree species. With the process-based simulation model Gotilwa applied to a *Q. ilex*
354 coppice in northeastern Spain, Gracia et al. (1999) predicted a *CUE* of 0.41. In contrast,
355 Luysaert et al. (2007) derived a surprisingly high value of 0.54 from a global database for
356 their so-called “Mediterranean warm evergreen” biome (table 2).

357 The low ecosystem *CUE* observed at our site (around 0.40) could be due to the ancient
358 management of the ecosystem as a coppice. The large belowground biomass and respiratory
359 maintenance costs associated to this management system may alter C-use rules and constrain
360 *CUE* compared to more productive tall forests (Salomón et al., 2013). Furthermore, relatively
361 high R_{aa} (see below), could be associated to the role of above-ground organs in storing
362 nitrogen and nonstructural carbohydrates. One-year old leaves act as reservoirs contributing to
363 spring shoot growth (Cherbuy et al., 2001) while stumps and stems contain large amount of
364 parenchyma helping the tree to resprout after perturbations. Accurately quantifying the
365 relative importance of respiratory sources is an important step towards understanding the
366 whole C budget. Under the steady-state assumption of Eq. 9 (Raich and Nadelhoffer
367 1989)(Raich and Nadelhoffer, 1989), our values of *GPP*, *ANPP* and R_{aa} resulted in
368 $TBCF = 670 \text{ g C m}^{-2} \text{ yr}^{-1}$. R_{aa} was $460 \text{ g C m}^{-2} \text{ yr}^{-1}$, a value estimated from leaf respiration and
369 stem CO_2 efflux measurements made at our site and upscaled to the stand (Rodríguez-

370 Calcerrada et al., 2011; Rodriguez-Calcerrada et al., 2014). Applying the same *TBCF*
371 approach to the Misson et al. (2010) data of soil respiration for the wet 2004 year yielded a
372 *TBCF* of $630 \text{ g C m}^{-2} \text{ yr}^{-1}$. With our estimate of $BNPP = 270 \text{ g C m}^{-2} \text{ yr}^{-1}$, the R_{ab} ranged
373 between 360 and $400 \text{ g C m}^{-2} \text{ yr}^{-1}$. Finally, we could deduct an R_h ranging between 210 and
374 $230 \text{ g C m}^{-2} \text{ yr}^{-1}$ by summing the three respiration components to reach the whole-ecosystem
375 respiration R_{eco} . For comparison, the meta-analysis of Litton and Giardina (2008) report a
376 *TBCF* of $705 \text{ g C m}^{-2} \text{ yr}^{-1}$ and a *BNPP* of $334 \text{ g C m}^{-2} \text{ yr}^{-1}$, and Rodeghiero and Cescatti
377 (2006) measured, in a more mesic *Quercus ilex* coppice in which the soil respiration is very
378 high ($1079 \text{ g C m}^{-2} \text{ yr}^{-1}$), a *TBCF* of $564 \text{ g C m}^{-2} \text{ yr}^{-1}$ with the two belowground respiration
379 components R_{ab} and R_h being equal.

380

381 ***4.2. Sensitivity of carbon use and partitioning to between-year variation in water*** 382 ***limitation.***

383 To characterize year to year variations in drought severity we used a long-term cumulated
384 water stress index, the *WSI*. This concept likely originated in (Schulze et al., 1980a; Schulze
385 et al., 1980b) who related changes in normalized maximal assimilation rates and daily carbon
386 gain with the sum of water stress obtained by cumulating daily pre-dawn water potentials
387 from the day of the last rainfall to the day under consideration. Later, Wullschleger and
388 Hanson (2006) did the same with transpiration rates from trees growing in a throughfall
389 displacement experiment. This cumulated water-stress, called water-stress integral or *WSI* by
390 Myers (1988), has been applied to predict growth processes occurring at longer time scales
391 such as canopy development, litter fall dynamic and tree radial growth (Benson et al., 1992;
392 Raison et al., 1992a; Raison et al., 1992b). In our study we demonstrated that *WSI* was
393 significantly related to the current year reproductive effort, secondary growth and all
394 ecosystem C fluxes (see also Arneth et al., 1998), and useful in explaining how the previous
395 year drought limitation affected the leaf production in the subsequent year.

396 *GPP*, R_{eco} and *NEP* were largely impacted by water limitation. The decline of *GPP*
397 with drought has been observed in our site at different time and space scales. At a seasonal
398 time scale, Limousin et al. (2010) intensively discussed how leaf photosynthetic limitations
399 were related to predawn water potential. At a daily time scale, *GPP* estimated from eddy
400 correlation fluxes was related to predawn water potential (Rambal et al., 2003). The *ANPP*
401 components have also been shown to be impacted by drought severity, with a hierarchy of
402 responses going from the more affected, the stem, to the less affected, the leaves (Table 1).
403 The larger sensitivity of stem growth validates the hypothesis of the Forest-BGC model (Hoff

404 et al., 2002) in which trees allocate C first to leaves and fine roots, for maximizing
405 productivity while minimizing water stress, and then to stems, which appears as an end-
406 product built with remaining C. The reproductive effort also declined significantly with
407 increasing drought, although it represented a smaller C use. Acorn production, the larger
408 component of reproduction, has been shown to be influenced by water availability during the
409 fruiting process, in particular during the initial (spring) and advanced (summer) stages of the
410 maturation cycle (Pérez-Ramos et al., 2010).

411 The leaf production was not related to the current-year *WSI* but to the previous year *WSI*.
412 Limousin et al. (2012) observed that in *Q. ilex* the leaf litterfall was also positively correlated
413 with the previous year *WSI* so that more leaves were shed and replaced following wet years
414 than following dry years. This phenomenon might be explained by the cost-benefit hypothesis
415 (Chabot and Hicks, 1982; Kikuzawa, 1991): if the leaf carbon assimilation is reduced by
416 water limitation during a dry year, the leaf life span should increase for the leaf lifetime
417 carbon gain to pay back the leaf construction cost, and thus fewer new leaves need to be
418 produced to maintain the *LAI*. This results in an alternation of years with high leaf production
419 /shedding following wet years and years of opposite characteristics, as commonly observed in
420 evergreen species and in particular in *Q. ilex* (Montserrat-Marti et al., 2009; Ogaya and
421 Penuelas, 2006; Rapp, 1969). Such a mechanism may also contribute to maintain the water
422 transport capacity of *Q. ilex* under long lasting drought as proposed by Martin-StPaul et al.
423 (2013). Current-year drought causes *GPP* and less so *NPP* to decline, so that *CUE* declines
424 slightly. In a wet year following a drier one, *CUE* could decline because $ANPP_{stem}$ would be
425 ruled by current climate and would be high as corresponds to a wet year, while leaves would
426 be produced in fewer amounts due to one-year-lag effect of drought on leaf production and
427 *CUE* could decline. Further researches could be necessary to quantify such carry-over effect
428 on *CUE*. Perhaps the strategy of *Q. ilex* to buffer the hydraulic system from climatic extremes
429 has a penalty on *CUE*.

430 Based on the responses to drought of the different compartments and on the
431 assumptions stated above (see Materials & Methods) we calculated the yearly *CUE* response
432 to drought (Fig. 7a). *CUE* slightly decreased with drought from 0.419 at $WSI = -100$ MPa day
433 to 0.373 at $WSI = -400$ MPa day. Interestingly, *CUE* declined at a slower rate than *GPP* and
434 *NPP* in response to water deficit (Fig. 7a). Maseyk et al. (2008) reported a constant *CUE* of
435 0.4 in a *Pinus halepensis* forest growing in a semi-arid Mediterranean-type climate and
436 proposed that acclimation of maintenance respiration to dry conditions could help maintaining
437 *CUE* and productivity relatively high under such water limited climate. Recent studies at our

438 site showed that respiration rates declined exponentially in both leaves and stems as tree water
439 availability decreased through summer months (Rodríguez-Calcerrada et al., 2011;
440 Rodríguez-Calcerrada et al., 2014). Based on the relationships between leaf/shoot predawn
441 water potential and leaf/stem respiration we calculated that stem and foliage CO₂ efflux
442 declined by 4.7% and 7.1%, respectively, for an increase of drought severity of
443 $WSI = 100$ MPa day. Altogether, acclimation of leaf, stem and root respiration to plant water
444 deficit buffers *NPP* sensitivity to drought and contributes to maintain *CUE* relatively constant
445 across years of widely different rainfall and vegetation stress. The ultimate reasons for such
446 reduction in respiration rates are still unclear, but it appears that reduced demand of
447 respiratory products from growth and maintenance processes may cause a down-regulation of
448 mitochondrial activity (Atkin and Macherel, 2009).

449 Besides reductions in autotrophic respiration, changes in R_h contribute to complicate
450 our understanding of the impact of drought on the whole ecosystem C sink strength. In trees,
451 acclimation refers to strictly physiological processes; while in soils changes in R_h refer to
452 ecosystem-level phenomenon potentially driven by multiple mechanisms including substrate
453 depletion, changing microbial community composition, and physiological changes.
454 Substantial questions remain about its response to soil water status, the interactions with
455 substrate quality, and the role of the top soil drying-rewetting cycles (Wei et al., 2010). The
456 course of soil water content at time scales shorter than the season is not necessarily correlated
457 to the *WSI*. In Mediterranean-type ecosystems, R_h is likely more influenced by an
458 unpredictable supply of substrate to the rhizosphere than by changes in the microbial
459 community or its efficiency (Curiel Yuste et al., 2014). Finally we suggest as Hopkins et al.
460 (2013) did that substrate availability *sensu lato*, including *GPP* and storage of nonstructural C
461 pool (neglected here), may be the ultimate driver of the two respiration fluxes.

462

463 **5. CONCLUSIONS**

464 Comparative measures of ecosystem fluxes and production components across 11 years of
465 contrasting water limitations in a *Q. ilex* stand help to better understand how Mediterranean-
466 type forest ecosystems will respond to the ongoing climate change and to better project future
467 C sequestration capacity.

468 We observed a clear effect of water availability in limiting all the ecosystem fluxes
469 *GPP*, R_{eco} and *NEP*, and that the drought-induced decline in R_{eco} dampens the decline of the
470 ecosystem C sequestration under drought conditions. In parallel, all the growth components

471 were found to be affected by water limitation, with a partition of *GPP* into tissues that tends
472 to minimize the negative impacts of drought on growth. An important result is that all the
473 changes followed the same trajectory as water stress varied over a large range of conditions,
474 from a wet year to a dry year occurring only once every 67 years. We did not observe any
475 tipping point or discontinuity in the C partitioning pattern. On average, only 40% of the
476 carbon assimilated as gross photosynthesis was used to construct new tissues, with the
477 remaining 60% being respired back to the atmosphere as autotrophic respiration. This low
478 ecosystem *CUE* could be inherited from the ancient management of the ecosystem as a
479 coppice and its large amount of standing belowground biomass.

480 There are several ecological issues that question the values of the estimated C fluxes
481 and their changes with increasing drought severity. It appeared in our case that autotrophic
482 respiration by trees and heterotrophic respiration by soil microorganisms are primarily
483 responsible for mediating the larger part of the carbon exchanges between the biosphere and
484 atmosphere. Climate changes and projected increasing dryness have the potential to influence
485 the activity of trees regulating exchanges among the carbon pools. Functional ‘down-
486 regulation’ or acclimation of plant respiration could reduce the respiratory autotrophic loss of
487 ecosystems, but unlike plant components, the existence of this phenomenon in heterotrophic
488 respiration remains more controversial (Harmon et al., 2011; Wieder et al., 2013). Current
489 models can simulate *GPP* relationships with autotrophic fluxes in a warmer environment
490 (Piao et al., 2010; Wythers et al., 2013), yet the parameterization of models able to capture the
491 apparent respiratory acclimation of both R_a and R_h to water limitation of ecosystems is an
492 emerging challenge for the modeling and flux research communities. We suggest that both
493 communities should adopt a bottom-up approach to advance our understanding at tissue, tree
494 and ecosystem scales to increasingly larger time and space scales.

495

496 *Acknowledgements.*

497 A doctoral research grant was provided by the French Environment and Energy Management
498 Agency (ADEME) to ML. Projects MIND (EVK2-CT-2002-000158), DROUGHT+ (ANR-
499 06-VULN-003-01) and CARBO-Extreme (FP7-ENV-2008-1-226701) contributed in partly
500 funding this research. The authors declare no conflict of interest in relation with this work.

501

502 **REFERENCES**

- 503 Ackerly, D.: Functional strategies of chaparral shrubs in relation to seasonal water deficit and
504 disturbance, *Ecological Monographs*, 74, 25-44, 2004.
- 505 Allard, V., Ourcival, J. M., Rambal, S., Joffre, R., and Rocheteau, A.: Seasonal and annual
506 variation of carbon exchange in an evergreen Mediterranean forest in southern France, *Glob.*
507 *Change Biol.*, 14, 714-725, 10.1111/j.1365-2486.2008.01539.x, 2008.
- 508 Arneeth, A., Kelliher, F., McSeveny, T., and Byers, J.: Net ecosystem productivity, net primary
509 productivity and ecosystem carbon sequestration in a *Pinus radiata* plantation subject to soil
510 water deficit, *Tree Physiol.*, 18, 785-793, 1998.
- 511 Atkin, O. K., and Macherel, D.: The crucial role of plant mitochondria in orchestrating
512 drought tolerance, *Annals of Botany*, 103, 581-597, 2009.
- 513 Aubinet, M., Grelle, A., Ibrom, A., Rannik, U., Noncrieff, J., Foken, T., Kowalski, A. S.,
514 Martin, P. H., Berbigier, P., Bernhofer, C., Clement, R., Elbers, J., Granier, A., Grunwald, T.,
515 Morgenstern, K., Pilegaard, K., Rebmann, C., Snijders, W., Valentini, R., and Vesala, T.:
516 Estimates of the annual net carbon and water exchange of forests: The EUROFLUX
517 methodology, *Adv. Ecol. Res.*, 30, 113-175, 2000.
- 518 Beer, C., Reichstein, M., Tomelleri, E., Ciais, P., Jung, M., Carvalhais, N., Rödenbeck, C.,
519 Arain, M. A., Baldocchi, D., Bonan, G. B., Bondeau, A., Cescatti, A., Lasslop, G., Lindroth,
520 A., Lomas, M., Luyssaert, S., Margolis, H., Oleson, K. W., Rouspard, O., Veenendaal, E.,
521 Viovy, N., Williams, C., Woodward, F. I., and Papale, D.: Terrestrial gross carbon dioxide
522 uptake: Global distribution and covariation with climate, *Science*, 329, 834-838,
523 10.1126/science.1184984, 2010.
- 524 Benson, M., Myers, B., and Raison, R.: Dynamics of stem growth of *Pinus radiata* as affected
525 by water and nitrogen supply, *Forest ecology and management*, 52, 117-137, 1992.
- 526 Bonan, G. B.: Forests and climate change: forcings, feedbacks, and the climate benefits of
527 forests, *science*, 320, 1444-1449, 2008.
- 528 Brouwer, R.: Distribution of dry matter in the plant, *Neth. J. Agric. Sci.*, 10, 361-376, 1962.
- 529 Campbell, G. S.: *Soil physics with basic: Transport models for soil-plant systems*, Elsevier,
530 1985.
- 531 Canadell, J., and Roda, F.: Root biomass of *Quercus ilex* in a montane Mediterranean forest,
532 *Canadian Journal of Forest Research*, 21, 1771-1778, 1991.
- 533 Chabot, B. F., and Hicks, D. J.: The ecology of leaf life spans, *Annual Review of Ecology and*
534 *Systematics*, 13, 229-259, 1982.
- 535 Cherbuy, B., Joffre, R., Gillon, D., and Rambal, S.: Internal remobilization of carbohydrates,
536 lipids, nitrogen and phosphorus in the Mediterranean evergreen oak *Quercus ilex*, *Tree*
537 *Physiol.*, 21, 9-17, 2001.
- 538 Clarke, P. J., Lawes, M. J., and Midgley, J. J.: Resprouting as a key functional trait in woody
539 plants—challenges to developing new organizing principles, *New Phytol.*, 188, 651-654, 2010.
- 540 Curiel Yuste, J., Fernandez-Gonzalez, A., Fernandez-Lopez, M., Ogaya, R., Penuelas, J.,
541 Sardans, J., and Lloret, F.: Strong functional stability of soil microbial communities under
542 semiarid Mediterranean conditions and subjected to long-term shifts in baseline precipitation,
543 *Soil Biology and Biochemistry*, 69, 223-233, 2014.
- 544 DeLucia, E. H., Drake, J. E., Thomas, R. B., and Gonzalez-Meler, M.: Forest carbon use
545 efficiency: is respiration a constant fraction of gross primary production?, *Glob. Change Biol.*,
546 13, 1157-1167, 10.1111/j.1365-2486.2007.01365.x, 2007.
- 547 Djema, A.: Cuantificación de la biomasa y mineralomasa subterránea de un bosque de
548 *Quercus ilex L.*, MSc thesis, Instituto Agronómico Mediterráneo, Zaragoza, España, 78 p. pp.,
549 1995.

550 Eckardt, F., Heim, G., Methy, M., and Sauvezon, R.: Interception de l'énergie rayonnante,
551 échanges gazeux et croissance dans une forêt méditerranéenne à feuillage persistant
552 (*Quercetum ilicis*), *Photosynthetica*, 9, 1975.

553 Fatichi, S., Leuzinger, S., and Körner, C.: Moving beyond photosynthesis: from carbon source
554 to sink-driven vegetation modeling, *New Phytol.*, 2013.

555 Franklin, O., Johansson, J., Dewar, R. C., Dieckmann, U., McMurtrie, R. E., Brännström, Å.,
556 and Dybzinski, R.: Modeling carbon allocation in trees: a search for principles, *Tree Physiol.*,
557 32, 648-666, 2012.

558 Gifford, R. M.: Plant respiration in productivity models: conceptualisation, representation and
559 issues for global terrestrial carbon-cycle research, *Functional Plant Biology*, 30, 171-186,
560 2003.

561 Giorgi, F.: Climate change hot-spots, *Geophysical Research Letters*, 33, 2006.

562 Gracia, C. A., Tello, E., Sabaté, S., and Bellot, J.: GOTILWA: An integrated model of water
563 dynamics and forest growth, in: *Ecology of Mediterranean evergreen oak forests*, Springer,
564 163-179, 1999.

565 Grote, R., Lavoie, A.-V., Rambal, S., Staudt, M., Zimmer, I., and Schnitzler, J.-P.: Modelling
566 the drought impact on monoterpene fluxes from an evergreen Mediterranean forest canopy,
567 *Oecologia*, 160, 213-223, 2009.

568 Grünzweig, J., Lin, T., Rotenberg, E., Schwartz, A., and Yakir, D.: Carbon sequestration in
569 arid-land forest, *Glob. Change Biol.*, 9, 791-799, 2003.

570 Harmon, M. E., Bond-Lamberty, B., Tang, J., and Vargas, R.: Heterotrophic respiration in
571 disturbed forests: A review with examples from North America, *Journal of Geophysical*
572 *Research: Biogeosciences* (2005–2012), 116, 2011.

573 Hoerling, M., Eischeid, J., Perlwitz, J., Quan, X., Zhang, T., and Pegion, P.: On the increased
574 frequency of Mediterranean drought, *Journal of Climate*, 25, 2146-2161, 10.1175/JCLI-D-11-
575 00296.1, 2011.

576 Hoff, C., Rambal, S., and Joffre, R.: Simulating carbon and water flows and growth in a
577 Mediterranean evergreen *Quercus ilex* coppice using the FOREST-BGC model, *Forest*
578 *Ecology and Management*, 164, 121-136, 10.1016/s0378-1127(01)00605-3, 2002.

579 Hoff, C., and Rambal, S.: An examination of the interaction between climate, soil and leaf
580 area index in a *Quercus ilex* ecosystem, *Ann. For. Sci.*, 60, 153-161, 2003.

581 Hopkins, F., Gonzalez-Meler, M. A., Flower, C. E., Lynch, D. J., Czimczik, C., Tang, J., and
582 Subke, J. A.: Ecosystem-level controls on root-rhizosphere respiration, *New Phytol.*, 199,
583 339-351, 2013.

584 Iwasa, Y., and Kubo, T.: Optimal size of storage for recovery after unpredictable
585 disturbances, *Evolutionary ecology*, 11, 41-65, 1997.

586 Jackson, R. B., Mooney, H., and Schulze, E.-D.: A global budget for fine root biomass,
587 surface area, and nutrient contents, *Proceedings of the National Academy of Sciences*, 94,
588 7362-7366, 1997.

589 Jaeger, E. B., and Seneviratne, S. I.: Impact of soil moisture–atmosphere coupling on
590 European climate extremes and trends in a regional climate model, *Climate Dynamics*, 36,
591 1919-1939, 10.1007/s00382-010-0780-8, 2011.

592 Kikuzawa, K.: A cost-benefit analysis of leaf habit and leaf longevity of trees and their
593 geographical pattern, *American Naturalist*, 138, 1250-1263, 1991.

594 Kjellström, E., Thejll, P., Rummukainen, M., Christensen, J. H., Boberg, F., Christensen, O.
595 B., and Maule, C. F.: Emerging regional climate change signals for Europe under varying
596 large-scale circulation conditions, *Climate Research*, 56, 103-119, 2013.

597 Leuzinger, S., and Quinn Thomas, R.: How do we improve Earth system models? Integrating
598 Earth system models, ecosystem models, experiments and long-term data, *New Phytol.*, 191,
599 15-18, 2011.

600 Limousin, J.-M., Longepierre, D., Huc, R., and Rambal, S.: Change in hydraulic traits of
601 Mediterranean *Quercus ilex* subjected to long-term throughfall exclusion, *Tree Physiol.*, 30,
602 1026-1036, 10.1093/treephys/tpq062, 2010.

603 Limousin, J. M., Rambal, S., Ourcival, J. M., Rodriguez-Calcerrada, J., Perez-Ramos, I. M.,
604 Rodriguez-Cortina, R., Misson, L., and Joffre, R.: Morphological and phenological shoot
605 plasticity in a Mediterranean evergreen oak facing long-term increased drought, *Oecologia*,
606 169, 565-577, 10.1007/s00442-011-2221-8, 2012.

607 Litton, C., and Giardina, C.: Below-ground carbon flux and partitioning: Global patterns and
608 response to temperature, *Functional Ecology*, 22, 941-954, 2008.

609 Lloret, F., Siscart, D., and Dalmases, C.: Canopy recovery after drought dieback in holm-oak
610 Mediterranean forests of Catalonia (NE Spain), *Glob. Change Biol.*, 10, 2092-2099, 2004.

611 López-Moreno, J. I., Vicente-Serrano, S. M., Gimeno, L., and Nieto, R.: Stability of the
612 seasonal distribution of precipitation in the Mediterranean region: Observations since 1950
613 and projections for the 21st century, *Geophysical Research Letters*, 36, L10703,
614 10.1029/2009GL037956, 2009.

615 López, B., Sabaté, S., and Gracia, C.: Annual and seasonal changes in fine root biomass of a
616 *Quercus ilex* L. forest, *Plant and Soil*, 230, 125-134, 2001a.

617 López, B., Sabaté, S., and Gracia, C. A.: Vertical distribution of fine root density, length
618 density, area index and mean diameter in a *Quercus ilex* forest, *Tree Physiol.*, 21, 555-560,
619 10.1093/treephys/21.8.555, 2001b.

620 Luo, Y., Melillo, J., Niu, S., Beier, C., Clark, J. S., Classen, A. T., Davidson, E., Dukes, J. S.,
621 Evans, R. D., Field, C. B., Czimczik, C. I., Keller, M., Kimball, B. A., Kueppers, L. M.,
622 Norby, R. J., Pelini, S. L., Pendall, E., Rastetter, E., Six, J., Smith, M., Tjoelker, M. G., and
623 Torn, M. S.: Coordinated approaches to quantify long-term ecosystem dynamics in response
624 to global change, *Glob. Change Biol.*, 17, 843-854, 10.1111/j.1365-2486.2010.02265.x, 2011.

625 Luysaert, S., Inglima, I., Jung, M., Richardson, A. D., Reichstein, M., Papale, D., Piao, S. L.,
626 Schulze, E. D., Wingate, L., Matteucci, G., Aragao, L., Aubinet, M., Beer, C., Bernhofer, C.,
627 Black, K. G., Bonal, D., Bonnefond, J. M., Chambers, J., Ciais, P., Cook, B., Davis, K. J.,
628 Dolman, A. J., Gielen, B., Goulden, M., Grace, J., Granier, A., Grelle, A., Griffis, T.,
629 GrÜNwald, T., Guidolotti, G., Hanson, P. J., Harding, R., Hollinger, D. Y., Hutyra, L. R.,
630 Kolari, P., Kruijt, B., Kutsch, W., Lagergren, F., Laurila, T., Law, B. E., Le Maire, G.,
631 Lindroth, A., Loustau, D., Malhi, Y., Mateus, J., Migliavacca, M., Misson, L., Montagnani,
632 L., Moncrieff, J., Moors, E., Munger, J. W., Nikinmaa, E., Ollinger, S. V., Pita, G., Rebmann,
633 C., Rouspard, O., Saigusa, N., Sanz, M. J., Seufert, G., Sierra, C., Smith, M. L., Tang, J.,
634 Valentini, R., Vesala, T., and Janssens, I. A.: CO₂ balance of boreal, temperate, and tropical
635 forests derived from a global database, *Glob. Change Biol.*, 13, 2509-2537, 10.1111/j.1365-
636 2486.2007.01439.x, 2007.

637 Mäkelä, A.: Implications of the pipe model theory on dry matter partitioning and height
638 growth in trees, *Journal of Theoretical Biology*, 123, 103-120, 1986.

639 Martin-StPaul, N. K., Limousin, J. M., Vogt-Schilb, H., Rodríguez-Calcerrada, J., Rambal, S.,
640 Longepierre, D., and Misson, L.: The temporal response to drought in a Mediterranean
641 evergreen tree: comparing a regional precipitation gradient and a throughfall exclusion
642 experiment, *Glob. Change Biol.*, 19, 2413-2426, 2013.

643 Maseyk, K., GRÜNZEIG, J. M., Rotenberg, E., and Yakir, D.: Respiration acclimation
644 contributes to high carbon-use efficiency in a seasonally dry pine forest, *Glob. Change Biol.*,
645 14, 1553-1567, 2008.

646 Medlyn, B., and Dewar, R.: Comment on the article by RH Waring, JJ Landsberg and M.
647 Williams relating net primary production to gross primary production, *Tree Physiol.*, 19, 137-
648 138, 1999.

649 Misson, L., Rocheteau, A., Rambal, S., Ourcival, J.-M., Limousin, J.-M., and Rodriguez, R.:
650 Functional changes in the control of carbon fluxes after 3 years of increased drought in a
651 Mediterranean evergreen forest?, *Glob. Change Biol.*, 16, 2461-2475, 10.1111/j.1365-
652 2486.2009.02121.x, 2010.

653 Misson, L., Degueldre, D., Collin, C., Rodriguez, R., Rocheteau, A., Ourcival, J.-M., and
654 Rambal, S.: Phenological responses to extreme droughts in a Mediterranean forest, *Glob.*
655 *Change Biol.*, 17, 1036-1048, 10.1111/j.1365-2486.2010.02348.x, 2011.

656 Montserrat-Marti, G., Camarero, J. J., Palacio, S., Perez-Rontome, C., Milla, R., Albuixech,
657 J., and Maestro, M.: Summer-drought constrains the phenology and growth of two coexisting
658 Mediterranean oaks with contrasting leaf habit: implications for their persistence and
659 reproduction, *Trees-Structure and Function*, 23, 787-799, 10.1007/s00468-009-0320-5, 2009.

660 Myers, B. J.: Water stress integral—a link between short-term stress and long-term growth,
661 *Tree Physiol.*, 4, 315-323, 1988.

662 Oechel, W., and Lawrence, W.: Carbon allocation and utilization, in: *Resource Use by*
663 *Chaparral and Matorral*, edited by: Miller, P. C., *Ecological Studies*, Springer New York, 185-
664 235, 1981.

665 Ogaya, R., and Penuelas, J.: Contrasting foliar responses to drought in *Quercus ilex* and
666 *Phillyrea latifolia*, *Biologia Plantarum*, 50, 373-382, 2006.

667 Papale, D.: Towards a standardized processing of Net Ecosystem Exchange measured with
668 eddy covariance technique: algorithms and uncertainty estimation, 3, 571-583, 2006.

669 Pérez-Ramos, I. M., Ourcival, J. M., Limousin, J. M., and Rambal, S.: Mast seeding under
670 increasing drought: results from a long-term data set and from a rainfall exclusion experiment,
671 *Ecology*, 91, 3057-3068, 10.1890/09-2313.1, 2010.

672 Piao, S., Luysaert, S., Ciais, P., Janssens, I. A., Chen, A., Cao, C., Fang, J., Friedlingstein, P.,
673 Luo, Y., and Wang, S.: Forest annual carbon cost: a global-scale analysis of autotrophic
674 respiration, *Ecology*, 91, 652-661, 2010.

675 Quézel, P., and Médail, F.: *Ecologie et biogéographie des forêts du bassin méditerranéen*,
676 Elsevier, Paris, France, 571 p. pp., 2003.

677 Raich, J., and Nadelhoffer, K.: Belowground carbon allocation in forest ecosystems: global
678 trends, *Ecology*, 70, 1346-1354, 1989.

679 Raison, R., Khanna, P., Benson, M., Myers, B., McMurtrie, R., and Lang, A.: Dynamics of
680 *Pinus radiata* foliage in relation to water and nitrogen stress: II. Needle loss and temporal
681 changes in total foliage mass, *Forest ecology and management*, 52, 159-178, 1992a.

682 Raison, R., Myers, B., and Benson, M.: Dynamics of *Pinus radiata* foliage in relation to water
683 and nitrogen stress: I. Needle production and properties, *Forest Ecology and Management*, 52,
684 139-158, 1992b.

685 Rambal, S.: Les transferts d'eau dans le système sol-plante en région méditerranéenne
686 karstique: une approche hiérarchique, Paris 11, 1990.

687 Rambal, S.: The differential role of mechanisms for drought resistance in a Mediterranean
688 evergreen shrub: a simulation approach, *Plant, Cell & Environment*, 16, 35-44, 1993.

689 Rambal, S., and Debussche, G.: Water balance of Mediterranean ecosystems under a changing
690 climate, in: *Global change and Mediterranean-type ecosystems*, Springer, 386-407, 1995.

691 Rambal, S., Damesin, C., Joffre, R., Méthy, M., and Seen, D. L.: Optimization of carbon gain
692 in canopies of Mediterranean evergreen oaks, *Annales des sciences forestières*, 1996, 547-
693 560,

694 Rambal, S., Ourcival, J. M., Joffre, R., Mouillot, F., Nouvellon, Y., Reichstein, M., and
695 Rocheteau, A.: Drought controls over conductance and assimilation of a Mediterranean
696 evergreen ecosystem: scaling from leaf to canopy, *Glob. Change Biol.*, 9, 1813-1824, 2003.

697 Rambal, S., Joffre, R., Ourcival, J., Cavender-Bares, J., and Rocheteau, A.: The growth
698 respiration component in eddy CO₂ flux from a *Quercus ilex* mediterranean forest, Glob.
699 Change Biol., 10, 1460-1469, 2004.

700 Rambal, S.: Le paradoxe hydrologique des écosystèmes méditerranéens, Annales de la
701 Société d'Horticulture et d'Histoire Naturelle de l'Hérault, 61-67, 2011.

702 Rapp, M.: Production de litière et apport au sol d'éléments minéraux dans deux écosystèmes
703 méditerranéens: la forêt de *Quercus ilex* L. et la garrigue de *Quercus coccifera* L., Oecol.
704 Plant., 4, 377-410, 1969.

705 Reichstein, M., Falge, E., Baldocchi, D., Papale, D., Aubinet, M., Berbigier, P., Bernhofer, C.,
706 Buchmann, N., Gilmanov, T., and Granier, A.: On the separation of net ecosystem exchange
707 into assimilation and ecosystem respiration: review and improved algorithm, Glob. Change
708 Biol., 11, 1424-1439, 2005.

709 Rodeghiero, M., and Cescatti, A.: Indirect partitioning of soil respiration in a series of
710 evergreen forest ecosystems, Plant and soil, 284, 7-22, 2006.

711 Rodríguez-Calcerrada, J., Martin-StPaul, N. K., Lempereur, M., Ourcival, J.-M., Rey, M.-d.-
712 C., Joffre, R., and Rambal, S.: Stem CO₂ efflux and its contribution to ecosystem CO₂ efflux
713 decrease with drought in a Mediterranean forest stand, Agric. For. Meteorol., 195-196, 61-72,
714 2014.

715 Rodríguez-Calcerrada, J., Jaeger, C., Limousin, J. M., Ourcival, J. M., Joffre, R., and Rambal,
716 S.: Leaf CO₂ efflux is attenuated by acclimation of respiration to heat and drought in a
717 Mediterranean tree, Functional Ecology, 25, , 2011.

718 Ryan, M. G.: Tree responses to drought, Tree Physiol., 31, 237-239, 2011.

719 Sala, A., Piper, F., and Hoch, G.: Physiological mechanisms of drought-induced tree mortality
720 are far from being resolved, New Phytol., 186, 274-281, 2010.

721 Salomón, R., Valbuena-Carabaña, M., Gil, L., and González-Doncel, I.: Clonal structure
722 influences stem growth in *Quercus pyrenaica* Willd. coppices: Bigger is less vigorous, Forest
723 Ecology and Management, 296, 108-118, 2013.

724 Schulze, E. D., Hall, A. E., Lange, O. L., Evenari, M., Kappen, L., and Buschbom, U.: Long-
725 term effects of drought on wild and cultivated plants in the Negev desert. I Maximal rates of
726 net photosynthesis., Oecologia, 45, 11-18, 10.1007/BF00346700, 1980a.

727 Schulze, E. D., Lange, O. L., Evenari, M., Kappen, L., and Buschbom, U.: Long-term effects
728 of drought on wild and cultivated plants in the Negev deser. II Diurnal patterns of net
729 photosynthesis and daily carbon gain, Oecologia, 45, 19-25, 10.1007/BF00346701, 1980b.

730 Shinozaki, K., Yoda, K., Hozumi, K., and Kira, T.: A quantitative analysis of plant form;the
731 pipe model theory,1, Japanese Journal of Ecology, 14, 97-105, 1964.

732 Stauch, V. J., Jarvis, A. J., and Schulz, K.: Estimation of net carbon exchange using eddy
733 covariance CO₂ flux observations and a stochastic model, Journal of Geophysical Research:
734 Atmospheres, 113, D03101, 10.1029/2007JD008603, 2008.

735 Staudt, M., Rambal, S., Joffre, R., and Kesselmeier, J.: Impact of drought on seasonal
736 monoterpene emissions from *Quercus ilex* in southern France, Journal of Geophysical
737 Research: Atmospheres (1984–2012), 107, ACH 15-11-ACH 15-19, 2002.

738 Thornley, J.: Respiration, growth and maintenance in plants, 1970.

739 Valentine, H. T.: Tree-growth models: derivations employing the pipe-model theory, Journal
740 of theoretical biology, 117, 579-585, 1985.

741 Vesk, P. A., and Westoby, M.: Sprouting ability across diverse disturbances and vegetation
742 types worldwide, Journal of Ecology, 92, 310-320, 2004.

743 Vilagrosa, A., Hernández, E. I., Luis, V. C., Cochard, H., and Pausas, J. G.: Physiological
744 differences explain the co-existence of different regeneration strategies in Mediterranean
745 ecosystems, New Phytol., 201, 1277-1288, 10.1111/nph.12584, 2014.

746 Waring, R. H., Landsberg, J. J., and Williams, M.: Net primary production of forests: a
747 constant fraction of gross primary production?, *Tree Physiol.*, 18, 129-134,
748 10.1093/treephys/18.2.129, 1998.

749 Wei, W., Weile, C., and Shaopeng, W.: Forest soil respiration and its heterotrophic and
750 autotrophic components: Global patterns and responses to temperature and precipitation, *Soil*
751 *Biology and Biochemistry*, 42, 1236-1244, 2010.

752 Wieder, W. R., Bonan, G. B., and Allison, S. D.: Global soil carbon projections are improved
753 by modelling microbial processes, *Nature Climate Change*, 3, 909-912, 2013.

754 Wullschlegel, S. D., and Hanson, P. J.: Sensitivity of canopy transpiration to altered
755 precipitation in an upland oak forest: evidence from a long-term field manipulation study,
756 *Glob. Change Biol.*, 12, 97-109, 10.1111/j.1365-2486.2005.001082.x, 2006.

757 Wythers, K. R., Reich, P. B., and Bradford, J. B.: Incorporating temperature-sensitive Q10
758 and foliar respiration acclimation algorithms modifies modeled ecosystem responses to global
759 change, *Journal of Geophysical Research: Biogeosciences*, 118, 77-90, 2013.

760 Zavala, M.: A model of stand dynamics for holm oak-aleppo pine forests, in: *Ecology of*
761 *Mediterranean Evergreen Oak Forests*, edited by: Rodà, F., Retana, J., Gracia, C., and Bellot,
762 J., *Ecological Studies*, Springer Berlin Heidelberg, 105-117, 1999.

763

764 **TABLES**

765

766 **Table 1.** Parameters of the linear ordinary least-square regression lines between the water
767 stress integral *WSI* in MPa day and components of the ecosystem yearly C budget and
768 aboveground components of the productivity. α_{OLS} is the slope of the Y vs. X relationship.
769 *GPP*, *R_{eco}* and *NEP* are gross primary productivity, ecosystem respiration and net ecosystem
770 productivity respectively, in g C m⁻² yr⁻¹. The components of the aboveground productivity
771 for leaves, reproductive effort and stem *ANPP_{leaf}*, *ANPP_{reprod}* and *ANPP_{stem}* are also expressed
772 in g C m⁻² yr⁻¹

773

| Y versus X | $\alpha_{OLS} \pm SE$ | $\beta_{OLS} \pm SE$ | r^2 | F | p | n |
|--|-----------------------|----------------------|-------|------|-----------|----|
| GPP versus WSI | 1.91 ± 0.43 | 1675 ± 97.5 | 0.72 | 20.1 | 0.0021*** | 10 |
| R _{eco} versus WSI | 0.77±0.32 | 1144±72.5 | 0.42 | 5.8 | 0.042* | 10 |
| NEP versus WSI | 1.15 ± 0.20 | 531.3 ± 46.2 | 0.80 | 32.2 | 0.0005*** | 10 |
| ANPP _{leaf(t)} ^o versus WSI(t-1) | 0.41 ± 0.15 | 233.0 ± 34.6 | 0.52 | 7.5 | 0.03* | 9 |
| ANPP _{leaf(t)} ^o versus WSI(t) | -0.12 ± 0.19 | 116.1 ± 43.6 | 0.05 | 0.41 | 0.54ns | 9 |
| ANPP _{reprod} versus WSI | 0.10 ± 0.04 | 49.1 ± 8.8 | 0.48 | 7.2 | 0.027* | 10 |
| ANPP _{stem} versus WSI | 0.42 ± 0.10 | 162.9 ± 22.5 | 0.69 | 17.9 | 0.0029*** | 10 |

774

775 **Table 2.** Literature values of carbon use efficiencies (CUE) for a broad range of forests

776

| Ref. | Vegetation | CUE |
|------------------------|-------------------------------------|------------------|
| This work | <i>Quercus ilex</i> coppice | 0.40 (0.37-0.42) |
| Oechel & Lawrence 1981 | MTE spp. | 0.38 |
| Waring et al. 1998 | Broad range of forests (BRFs) | 0.47±0.04 |
| Medlyn & Dewar 1999 | BRFs | 0.31-0.59 |
| Gracia et al. 1999 | <i>Quercus ilex</i> coppice | 0.41 |
| De Lucia et al. 2007 | BRFs | 0.53(0.23-0.83) |
| Luyssaert et al. 2007 | Mediterranean warm evergreen | 0.54 |
| Litton & Giardina 2008 | BRFs | 0.43 |
| Luyssaert et al. 2009 | Temp. & boreal forests | 0.51±0.02 |
| Piao et al. 2010 | BRFs (MAT = 13°C) | 0.475 |
| Vica et al. 2012 | BRFs with low-nutrient availability | 0.42±0.02 |

777

778 **FIGURES**

779

780 **Fig 1.** Method used in closing the whole-ecosystem carbon balance. Arrows are the
781 information lines. The grey boxes surrounded by a continuous line are the ecosystem scale
782 flux measurements yielding NEP , GPP and R_{eco} values. The green boxes are the continuous
783 biometric measurements of the growth components. The boxes surrounded by a dashed line
784 mean discrete measurements. The brown boxes are discrete measurements of fluxes (from
785 leaf, stem and soil) up-scaled in time and space.

786

787 **Fig 2.** Scheme showing how the biometric estimate of NPP determines the partition of R_{eco} in
788 its components R_a and R_h . In this figure, we plot GPP , NEP and NPP at their average values.
789 The red arrow shows how error in estimating NPP propagates in R_a and R_h . All variables
790 expressed in $g\ C\ m^{-2}\ yr^{-1}$.

791

792 **Fig. 3.** Ordinary least-square regression lines between the water stress integral WSI and gross
793 primary productivity GPP (light grey circle) and net ecosystem productivity NEP (dark grey
794 circle). WSI is expressed in $MPa\ day$ and both GPP and NEP in $g\ C\ m^{-2}\ yr^{-1}$. 2005 data not
795 used in the analysis was also plotted (empty square for GPP and empty triangle for NEP).

796

797 **Fig. 4.** Ordinary least-square regression line between the water stress integral WSI and the net
798 productivity of stems (error bars are standard-deviation). WSI is expressed in $MPa\ day$ and
799 $ANPP_{stem}$ in $g\ C\ m^{-2}\ yr^{-1}$. 2005 data not used in the analysis was also plotted (empty triangle).

800

801 **Fig. 5.** Ordinary least-square regression line between the water stress integral WSI and the net
802 productivity of the reproductive effort (flowers and fruits; error bars are standard-deviation).
803 WSI is expressed in $MPa\ day$ and $ANPP_{reprod}$ in $g\ C\ m^{-2}\ yr^{-1}$. 2005 data not used in the analysis
804 was also plotted (empty triangle).

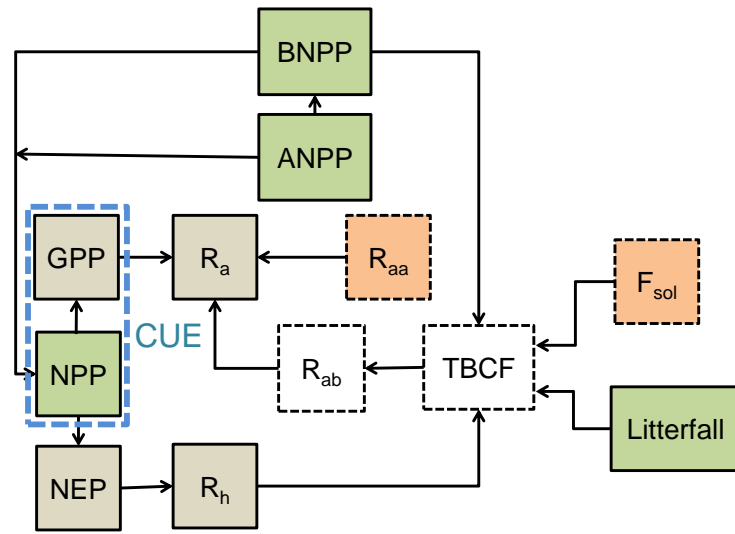
805

806 **Fig. 6.** Ordinary least-square regression lines between the aboveground net primary
807 productivity of leaves of the current year and (a) the water stress integral WSI of the previous
808 year (dark grey circle and standard-deviation), and (b) the water stress integral WSI of the
809 current year (empty circle and standard-deviation). WSI is expressed in $MPa\ day$ and $ANPP_{leaf}$
810 in $g\ C\ m^{-2}\ yr^{-1}$. 2005 data not used in the analysis was also plotted (empty triangle).

811

812 **Fig. 7.** (a) Change in the partition of gross primary productivity (*GPP*), expressed in g C m^{-2}
813 yr^{-1} , with increasing drought intensity (*WSI*), in MPa day. The red line displays the decline
814 of *GPP* with decreasing *WSI*. The net primary productivity (*NPP*) components are: perennial
815 aboveground + belowground parts (dark grey), reproductive effort (flowers and fruits;
816 medium grey), leaves and fine roots (light grey), all expressed in $\text{g C m}^{-2} \text{yr}^{-1}$. The dashed red
817 curve is for the carbon-use efficiency *CUE*. (b) Change in ecosystem respiration (R_{eco} , grey
818 line) and net ecosystem productivity (*NEP*, dark line), both in $\text{g C m}^{-2} \text{yr}^{-1}$, with increasing
819 drought intensity (*WSI*). The dashed orange line is for the R_a/GPP ratio and the dashed purple
820 line for the R_h/R_{eco} ratio.

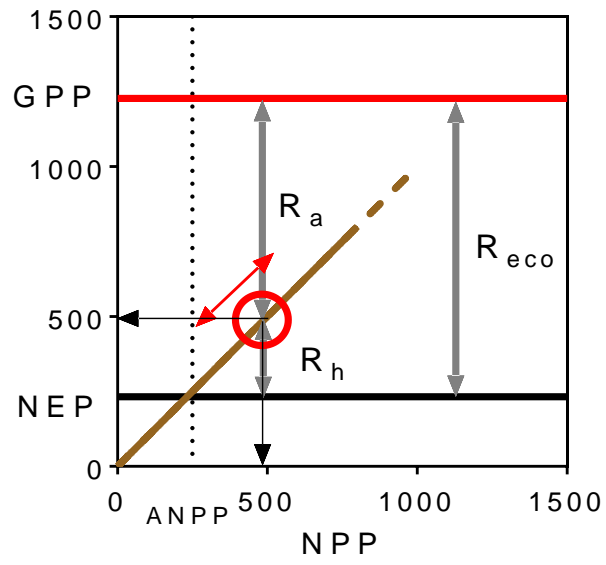
821 **Fig. 1.**



822

823

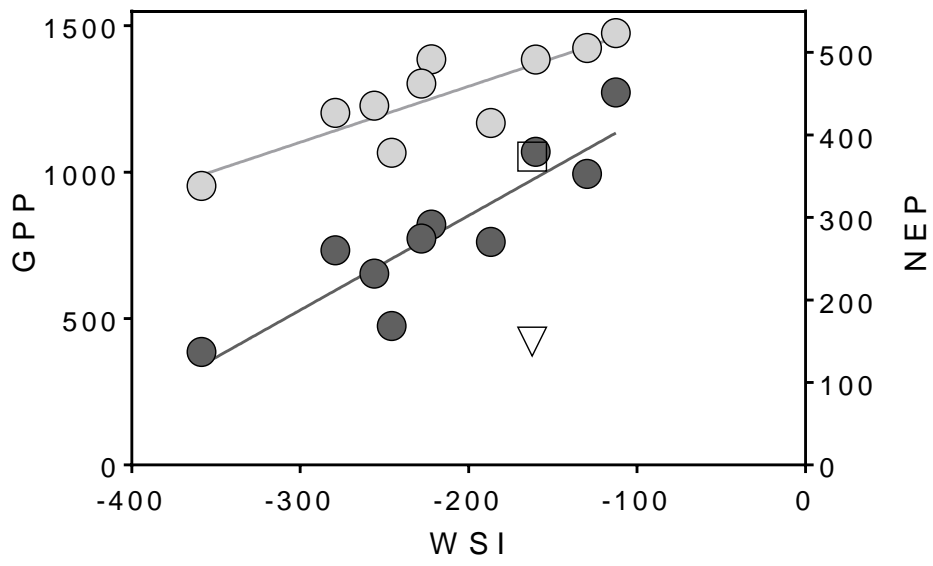
824 **Fig. 2.**



825

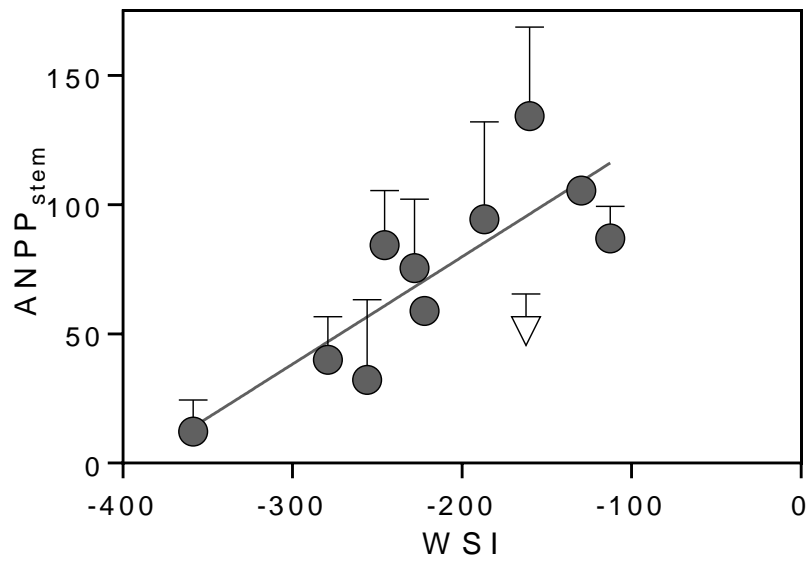
826

827 **Fig. 3.**



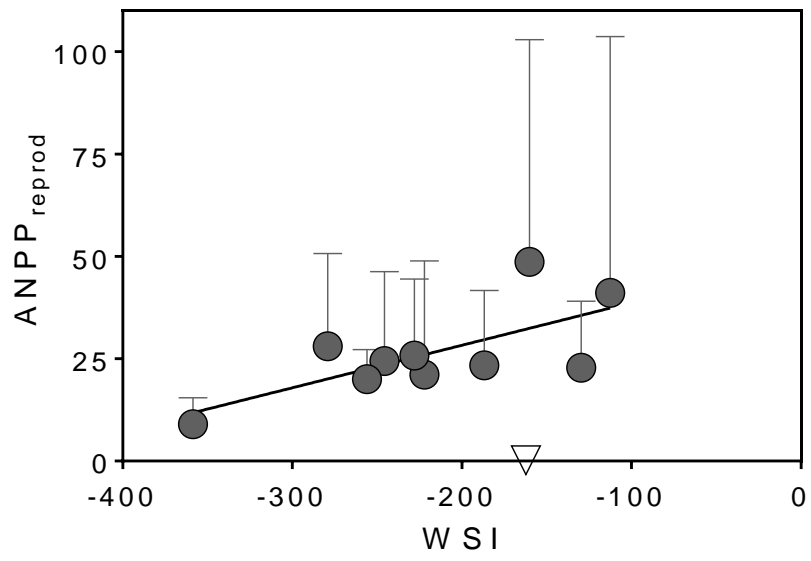
828

829 **Fig. 4.**

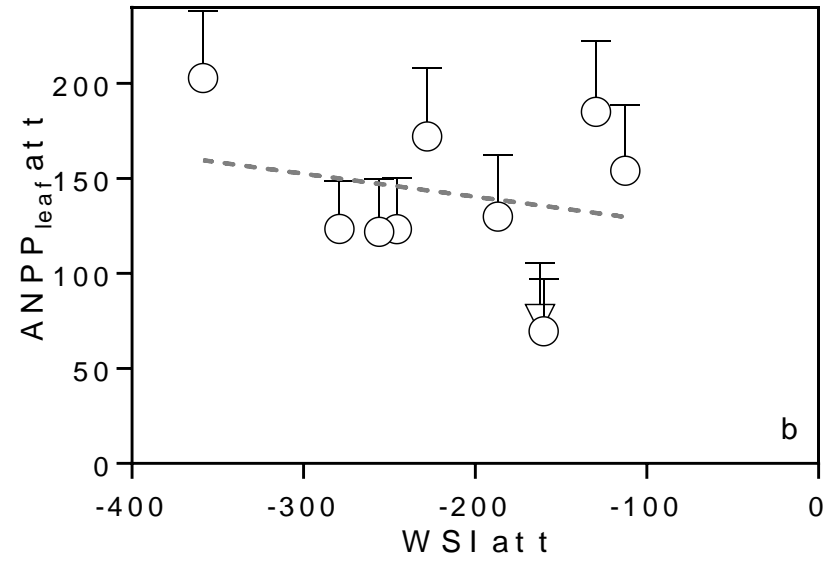
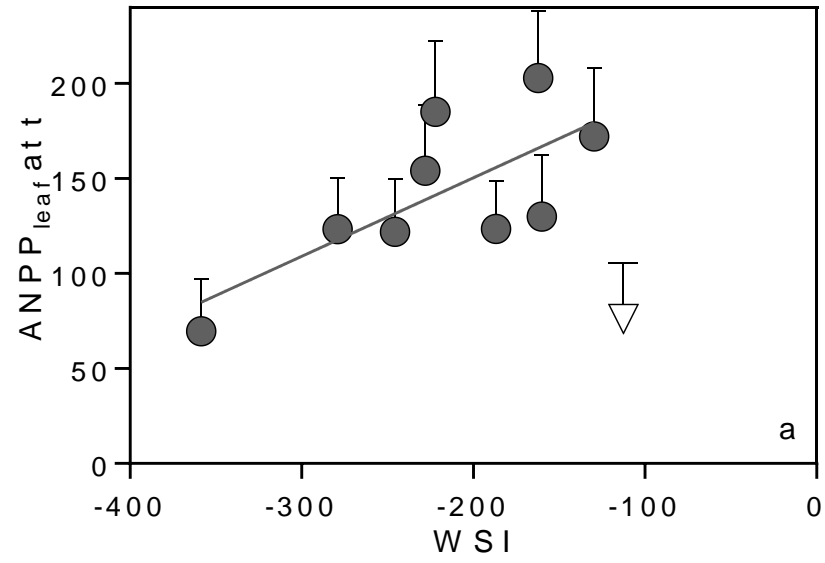


830

831 **Fig. 5.**



832 **Fig. 6.**



833

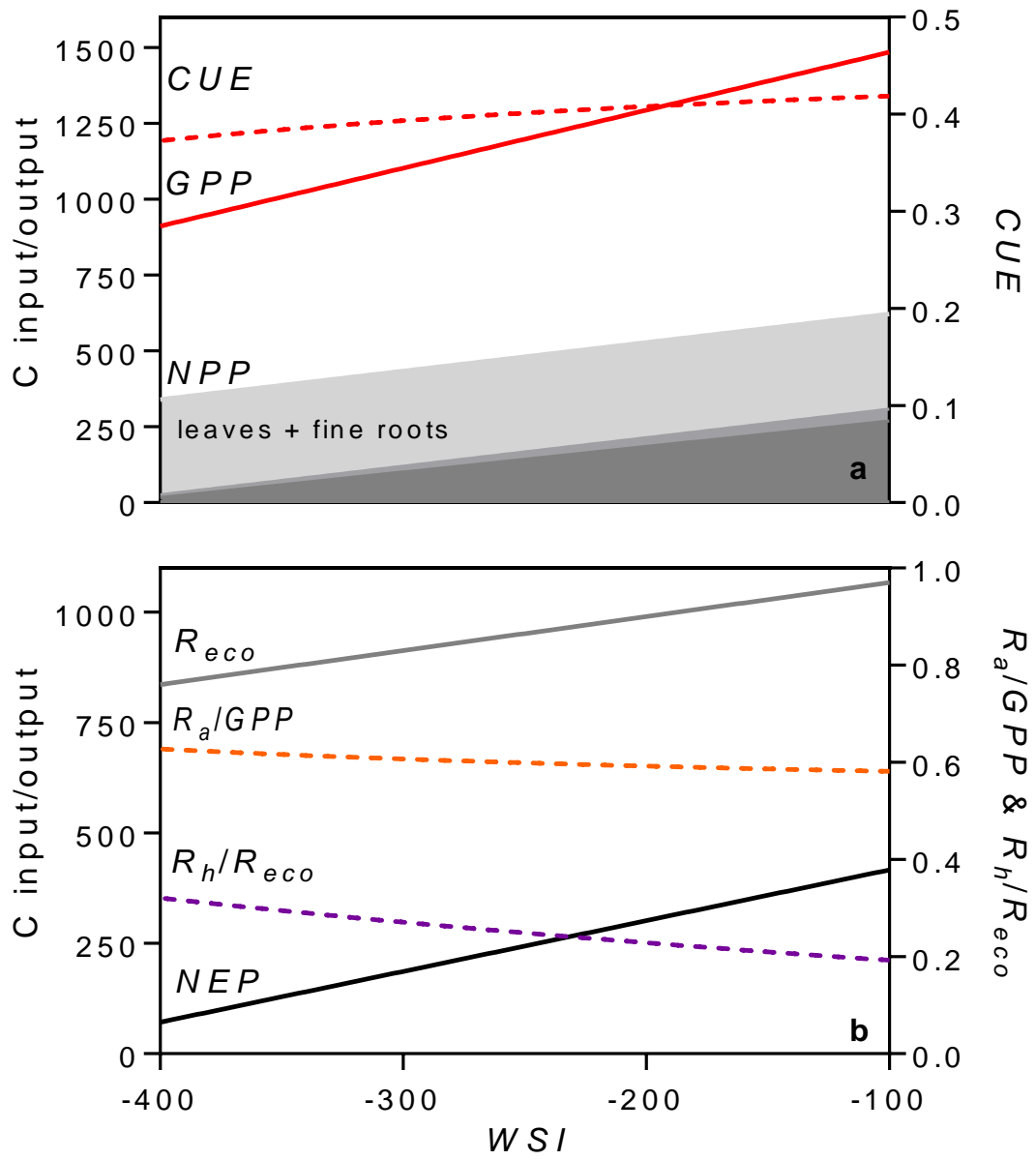
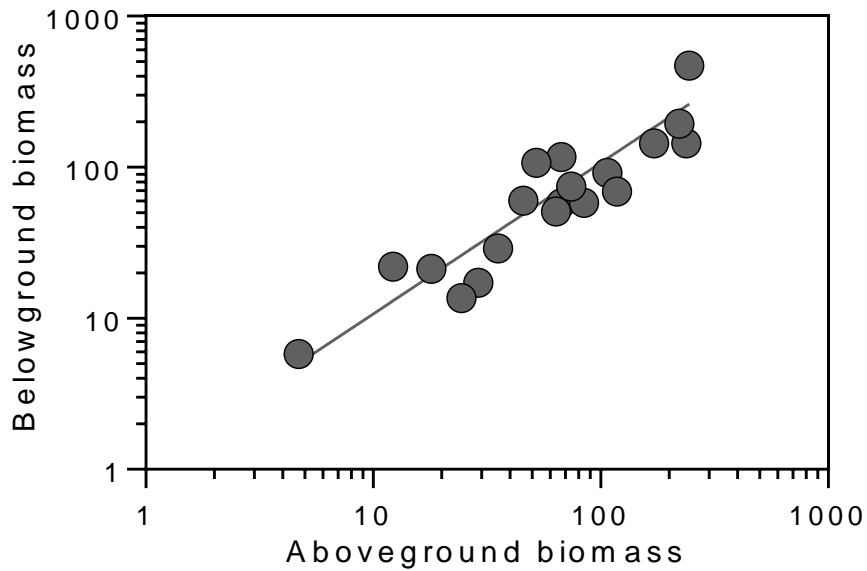
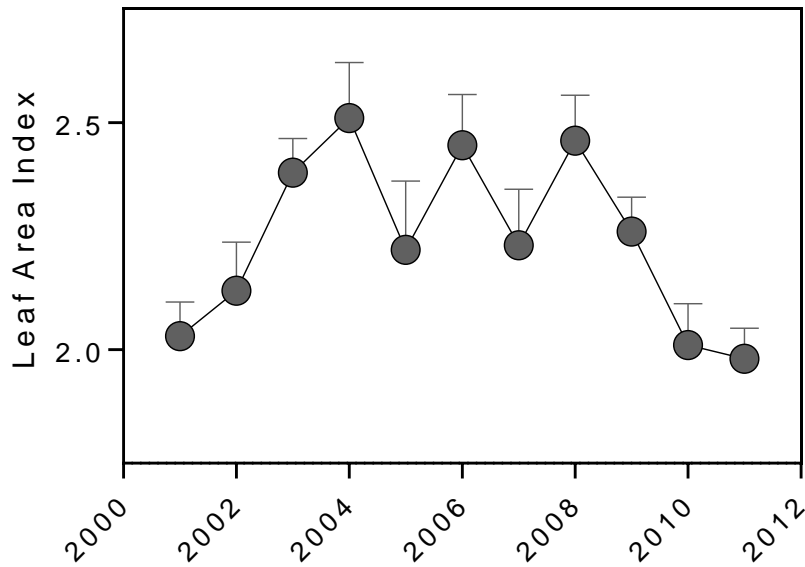


Fig. A1. Relationship between aboveground perennial biomass (g Dry Matter) and the corresponding belowground biomass (g Dry Matter). The belowground biomass is the sum of biomass values for root crown, roots greater than 5 cm, roots ranging from 1 to 5cm



diameter.

839 **Fig. A2.** Time course of the peak LAI derived from continuous measurements of half-hourly
840 f_{APAR} between 11 AM and 1 PM from DOY 205 to 225. The Stem Area Index SAI was
841 estimated by image processing of hemispheric photography and assumed constant for the
842 whole period and equal to 0.5. The relationship between leaf area index and water stress
843 integral (WSI) is statistically non-significant.



844